

Rock Burst Intensity Classification Based on the Radiated Energy with Damage Intensity at Jinping II Hydropower Station, China

Bing-Rui Chen · Xia-Ting Feng · Qing-Peng Li ·
Ru-Zhou Luo · Shaojun Li

Received: 5 September 2012 / Accepted: 20 November 2013 / Published online: 1 December 2013
© Springer-Verlag Wien 2013

Abstract Based on the radiated energy of 133 rock bursts monitored by a microseismic technique at the Jinping II hydropower station, in Sichuan province, China, we analyzed the advantages and disadvantages of qualitative classification methods for the rock burst intensity. Then, we investigated the characteristics, magnitude, and laws of the radiated energy, as well as the relationship between the rock burst radiated energy and intensity. Then, we selected the energy as an evaluation index for the rock burst intensity classification, and proposed a new rock burst intensity quantitative classification method, which utilized the hierarchical clustering analysis technique with the complete-linkage method. Next, we created a new set of criteria for the quantitative classification of the rock burst intensity based on radiated energy and surrounding rock damage severity. The new criteria classified the rock burst intensity into five levels: extremely intense, intense, moderate, weak, and none, and the common logarithms of the radiated energy of each level were $>7 \lg(E/J)$, $>4 \lg(E/J)$ and $<7 \lg(E/J)$, $>2 \lg(E/J)$ and $<4 \lg(E/J)$, $>1 \lg(E/J)$ and $<2 \lg(E/J)$, and $<1 \lg(E/J)$, respectively. Finally, we investigated the factors influencing the classification, and verified its feasibility and applicability via several practical rock burst examples.

Keywords Rock burst intensity classification · Microseismic monitoring · Radiated energy · Hierarchical clustering · Jinping

1 Introduction

Rock bursts are engineering disasters that often occur during underground excavation in high-stress, hard, brittle rock zones. They have been investigated extensively by many researchers (Canadian Rockburst Research Program 1996; Cook et al. 1966; He et al. 2010; Ortlepp and Stacey 1994; Tang 2000; Zhang et al. 2012a) and many significant advancements have been achieved. Although there have been few studies on rock burst intensity classification methods after the occurrence of rock bursts, representative rock burst intensity classification methods include: Russnes' method (Russnes 1974), which classifies the rock burst intensity into four levels (none, weak, moderate and severe rock bursts, according to the sound, shape and features of failure after the rock burst); Brauner's method (Brauner 1985), which classifies rock bursts into three grades based on the intensity of destruction to the surrounding rock mass; Tang's method (Tang 1992), which classifies rock bursts into four classifications in terms of a large number of laboratory tests and investigations in situ, and considers the mechanical characteristics, the type and the shape of the failure, the intensity of destruction and the sound of the rock burst; the Canadian Rockburst Research Program's (CRRP) (1996) method, which classifies the severity of rock burst damage into minor, moderate, and major damage, and estimates the severity of rock burst damage based on observations and empirical evidence or stress-to-strength ratios and geometric considerations; and the Code for Geological Investigations of Hydropower Engineering's

B.-R. Chen (✉) · X.-T. Feng · Q.-P. Li · S. Li
State Key Laboratory of Geomechanics and Geotechnical Engineering, Institute of Rock and Soil Mechanics, Chinese Academy of Sciences, 2# Xiaohongshan, Bayi Road, Wuhan, Hubei 430071, China
e-mail: brchen@whrsm.ac.cn

R.-Z. Luo
China Railway 13th Bureau Group CO., LTD,
Tianjin 300308, China

(CGIHE) method, proposed by the National Standards Compilation Group of the People's Republic of China (2008), which will be introduced in detail in Sect. 2.2.

These classification methods have been widely used in rock engineering and have aided in the prevention and control of rock bursts due to their simplicity and flexibility. However, because rock burst intensity levels using the methods above are classified according to the apparent characteristics of the rock burst occurrence, such as the type and shape of failure, the intensity of destruction, and the sound of the rock burst, these methods can only be used to evaluate rock burst intensity qualitatively and not quantitatively. Moreover, conflicts can occur among the different evaluation indexes, even when they use the same method. For example, a rock burst may be classified as an intense rock burst in terms of the depth and the shape of the rock burst failure zone by an engineer; however, it may also be ranked as a moderate rock burst on the basis of the rock burst sound by another engineer when the collapse is dominant. The different classification levels that can be obtained for the same rock burst by different engineers are an obvious disadvantage for the prevention and control of rock bursts. Thus, a new rock burst classification method is introduced in this paper for quantitatively evaluating rock burst intensity on the basis of the radiated energy of the rock burst, as monitored by a microseismic technique and surrounding rock damage severity.

In recent years, with the development of microseismic monitoring technology and analysis methods, the microseismic technique has become widely used in rock engineering (Milev et al. 2001; Young and Collins 2001; Ge 2005; Luo et al. 2010; Chen et al. 2011; Snelling et al. 2013), and thus, it is possible to use this technology to monitor the development process of and obtain the amount of radiated energy from a rock burst during the construction process in rock engineering. It is also possible to explore and accurately identify rock burst intensity classification criteria in terms of radiated energy.

In general, the three basic mechanisms of rock bursts, i.e., strain burst, fault-slip burst, and their combination, have been accepted (Board 1994; Tang 2000). Due to large-scale excavation, shear-rupture and fault-slip types of rock bursts are more possible in deep mining tunnels than in deep civil tunnel projects (Ortlepp and Stacey 1994). According to Tang (2000), the majority of rock bursts during civil tunnel constructions were of the strain type. There were 133 rock bursts recorded in detail in the microseismic monitoring zone, which is shown in Fig. 1, during the constructions of the headrace tunnels and the drainage tunnel of the Jinping II hydropower station in China. According to site observation and survey, all three types of rock bursts occurred in the deep tunnel projects of the Jinping II hydropower station, while strain rock bursts

were the most common. Based on these data, we first analyzed and discussed the advantages and disadvantages of the rock burst intensity qualitative classification, using the CGIHE method as an example. Second, we investigated the characteristics, magnitude and laws of radiated energy, and the relationship between the rock burst radiated energy, the intensity of destruction, and the supporting system of the surrounding rock mass. Then, a new rock burst intensity quantitative classification method, which utilizes the hierarchical clustering analysis technique, was introduced based on the radiated energy monitored by the microseismic technique as the rock burst occurred. Lastly, we determined a new set of criteria for rock burst intensity classification based on the radiated energy and surrounding rock damage severity, and verified its feasibility and applicability using several practical rock burst examples.

2 Background of the Proposed Rock Burst Intensity Classification Method

2.1 Project Introduction

The Jinping II hydropower station, which is located on the Great Jinping River Bend of Yalong River in Jinping, Liangshan Yi Autonomous Prefecture, Sichuan, takes advantage of the >310 m natural drop of the Jinping Yalong River Bend and diverts the water to headrace tunnels traveling through Jinping mountain instead of its original path, as shown in Fig. 1a. There are seven parallel tunnels in total and the length of a single tunnel is approximately 16.7 km. The percentage of the tunnels that are covered by rock mass with a thickness of over 1,500 m is approximately 75.7 %, and the maximum depth of the tunnels is approximately 2,525 m. This project was described in more detail by Wu et al. (2010).

High ground stress and strong rock bursts are the obvious characteristics of this area. Feng and Zhou (2006) suggested that when the overburden is over 1,200 m and farther from the Yalong River, the geostatic stress is dominant and the maximum principle stress is up to 63 MPa. The rock mass was mainly comprised of Baishan Group marble; its physical and mechanical properties are listed in Table 1 (Zhang et al. 2012b; Huang 2008). Its velocity, which was obtained using the back analysis method based on blasting information, ranges from 5,000 to 6,000 m/s. During the process of constructing the tunnels, rock bursts occurred frequently and caused significant problems in terms of safety (Shan and Yan 2010; Zhang et al. 2012a). Therefore, the microseismic technique was introduced to monitor induced seismic activity of the rock mass, in order to evaluate probable locations of rock bursts and thus reduce injuries to personnel and damage to equipment. Figure 1b and c show the

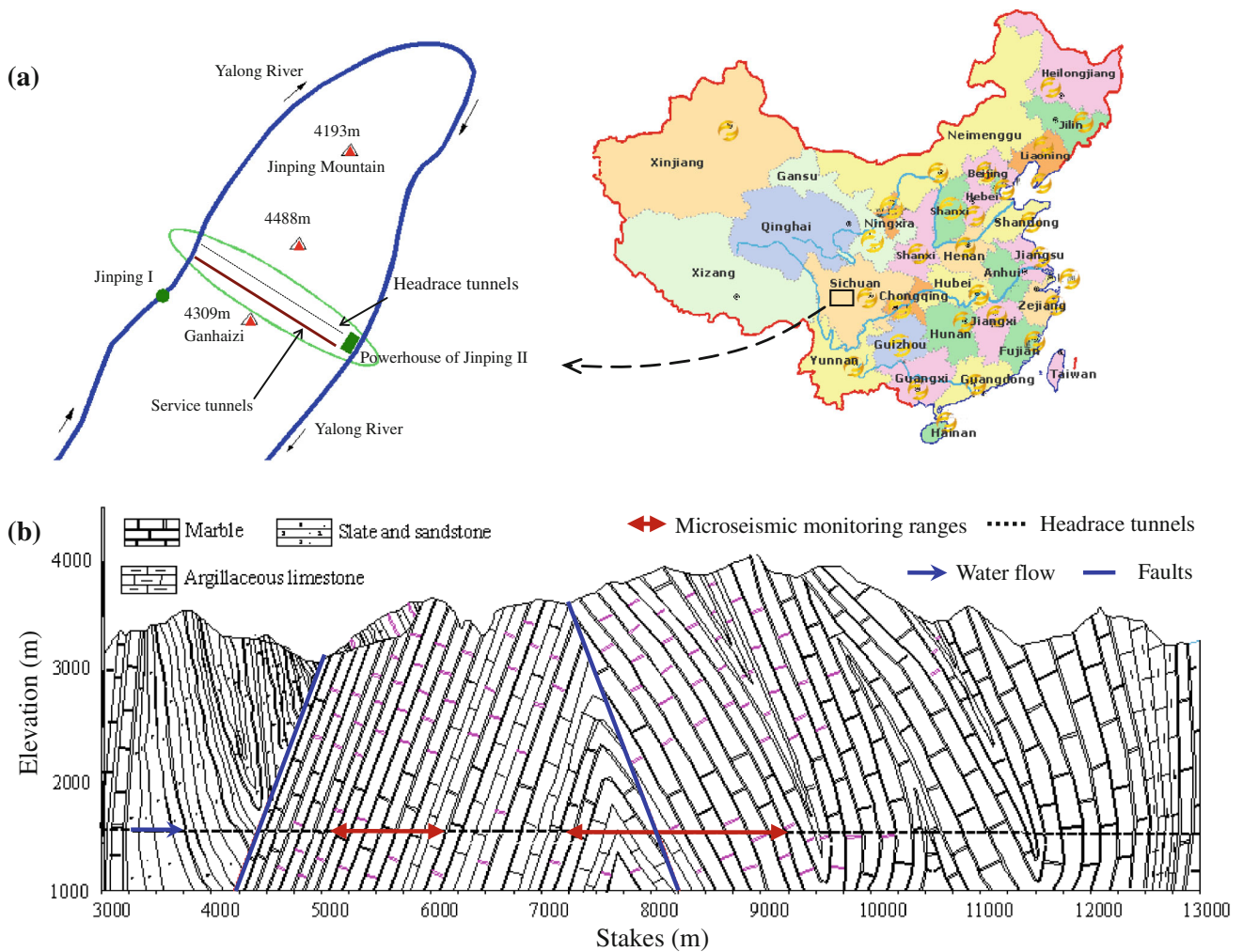


Fig. 1 Location of the Jinping II hydropower station and the ranges of microseismic monitoring: **a** location and plan of the Jinping II hydropower station (Jiang et al. 2010); **b** rock mass thickness covered and geological conditions in microseismic monitoring ranges; **c** ranges of microseismic monitoring and location of rock burst I, II, III, IV and V, which are K6 + 152–160, K8 + 805–815, K6 + 025–045, K8 + 827–852 and K5 + 623–628, respectively

(1[#], 2[#], 3[#] and 4[#] are the indexes of the 4 headrace tunnels, P[#] is the drainage tunnel, A[#] and B[#] are 2 traffic tunnels, and B-1[#], B-2[#] and B-3[#] are branches of traffic tunnel B[#] that were used to accelerate the construction of the four headrace tunnels. In the following drawings and text, the origin of all Stakes is at the western entrance of the 3[#] tunnel and the unit is meter.); **d** Distribution of sensors (unit: meter)

characteristics of the seven tunnels in which microseismic monitoring was conducted and the rockburst intensity was evaluated. They are covered by a 1,500–2,525-m-thick rock mass, and the total length of the tunnels combined is approximately 6.5 km.

2.2 Microseismic Monitoring

The microseismic data acquisition system, which allowed fast processing of seismic signals from many of the maximum 54 channels in the Jinping II project, was built based on the Integrated Seismic System (ISS) made in South Africa. The system has a signal-conditioning unit consisting of preamplifiers (0–60 dB), an anti-alias filter, and a 24-bit analog-to-digital conversion unit. The sampling

frequency was set to 6,000 Hz and recording data length was determined by trigger-start level and trigger-end level. The digitized signals were discriminated using the long-term averaging/short-term averaging (LTA/STA) method with a predefined triggering threshold. Only four geophone signals triggered the system “at the same time”, the data of which were all saved onto a hard disk. Each tunnel utilized a six-channel seismic data acquisition unit. Six channels were allocated to the two rows, the first and the second rows were 50–70 and 100–120 m away from tunnel face, respectively, and each row had the three uniaxial geophone sensors, as shown in Fig. 1d. The second row of the sensors was moved to a location 50–70 m away from the tunnel face when the first row of the sensors was 100–120 m away from the tunnel face. The seismic data acquisition unit and

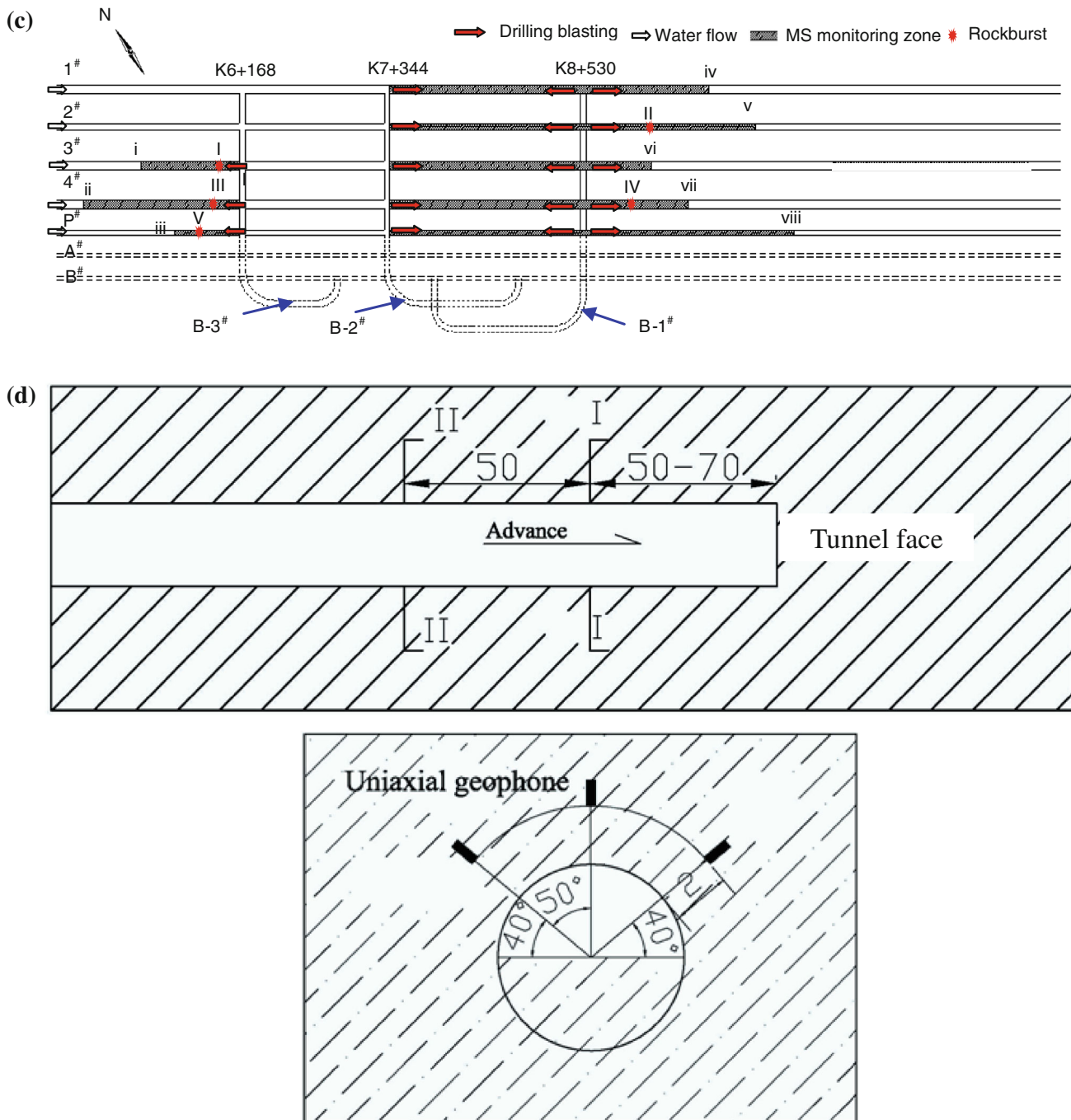


Fig. 1 continued

sensors were moved forward with the advancement of the tunnel face. The sensors, made in South Africa, had a natural frequency of 14 Hz and an approximate usable frequency range that varied from 7 to 2,000 Hz.

2.3 The Method of CGIHE and its Disadvantages

The CGIHE method was proposed by the National Standards Compilation Group of the People's Republic of

China, as described in detail in Table 2. Due to its simple and flexible operation, it was introduced to the construction process of the Jinping II hydropower station and provided considerable help in evaluating rock burst intensity.

When the tunnels were excavated in the microseismic monitoring zone, shown in Fig. 1c, 133 rock bursts were recorded in detail and classified into three levels using the CGIHE method on the basis of rock burst phenomena, which are listed in Table 2. The events included 18 intense,

Table 1 Physical and mechanical parameters for Jinping II Baishan Group marble (Zhang et al. 2012b; Huang 2008)

Parameters	Parameters value
Poisson’s ratio μ	0.21–0.33
Bulk weight γ	$2.5\text{--}2.8 \times 10^4 \text{ N m}^{-3}$
Uniaxial compression strength of saturated rock R_b	100–120 MPa
Maximum principle stress σ_m	46–70 Mpa
Depth of tunnels H	1,500–2,500 m

51 moderate and 64 weak rock bursts, as shown in Fig. 2. The common logarithms of the radiated energies of the intense, moderate, and weak rock bursts, as calculated by the energy attenuation formula along the traveling path of the wave (Kostrov 1974; Rudnicki and Freund 1981) based on the signals from the microseismic stations, were seen to vary from -0.49 to $7.61 \lg(E/J)$, from -0.92 to $7.01 \lg(E/J)$ and from -0.10 to $6.38 \lg(E/J)$, respectively. Their mean values of radiated energy were $3.52 \lg(E/J)$, $3.48 \lg(E/J)$, and $2.78 \lg(E/J)$, respectively. A clear law could not be seen between the rock burst intensity classification according to the CGIHE method and the radiated energy, as shown in Fig. 2.

Table 2 The CGIHE method

Rock burst levels	Phenomena	Classification standard	
		Critical depth (m)	UCS/ σ_m
Weak	Main failure type: slight spalling and slabbing in surface of surrounding rock mass; rock mass is not ejected; Sound: cracking sound can be heard occasionally; Depth of failure: less 0.5 m; Construction is not affected	$H \geq H_{cr}$	4–7
Moderate	Main failure type: severe spalling and slabbing of surrounding rock mass; rock mass is slightly ejected; Sound: cracking sound like a detonator blasting; slight cracking sound lasting for some time inside the rock mass; Depth of failure: more than 0.5 m and <1.0 m and failure range is obvious; Construction is barely affected		2–4
Intense	Main failure type: a great deal of rock mass is suddenly ejected with rock power; Sound: the failure sounds like an explosive blast; it is loud and lasts longer; Depth of failure: more than 1.0 and <3.0 m; failure range is extensive; Construction will be affected to some extent		1–2
Extremely intense	Main failure type: large block of rock mass is suddenly ejected with intensive seismicity; the stability of the whole carve is seriously affected; Sound: the failure sounds like thunder or a cannonball; it lasts a longer time; Depth of failure: more than 3.0 m; the failure range is larger and the size of the rock fragment is larger; Construction is seriously affected		<1

UCS uniaxial compressive strength

It remains unclear as to why the radiated energy of 8 of the 18 intense rock bursts was less than the average radiated energy of the 51 moderate and 64 weak rock bursts, and why the radiated energy of 17 of the 51 moderate rock bursts was less than the average radiated energy of the 64 weak rock bursts under the same radiation pattern assumption.

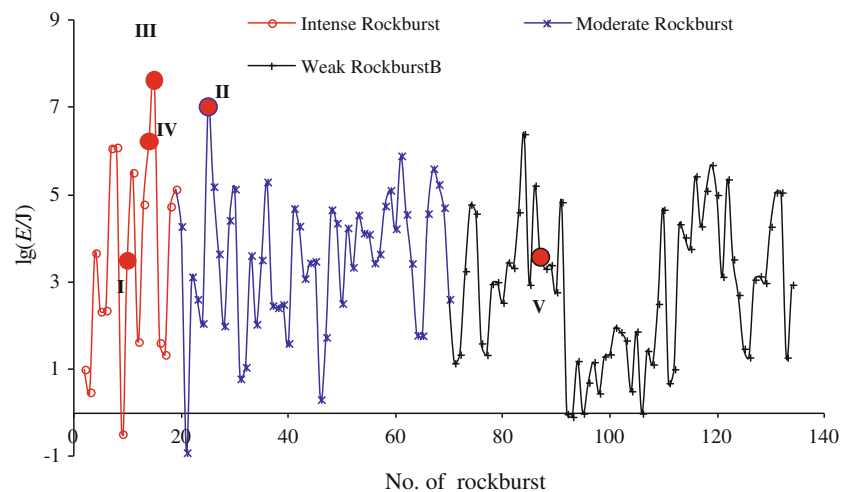
2.4 Discussion of the Qualitative Rock Burst Intensity Classification Method

How can the above conclusions be drawn? Intense rock burst I and moderate rock burst II, with locations and relationships between the radiated energy and the intensity levels shown in Figs. 1b, c and 2, respectively, are used below as examples to discuss the advantages and disadvantages of the CGIHE method, which is a typical qualitative rock burst intensity classification method.

2.4.1 Rock Burst Example I: An Intense Rock Burst According to the CGIHE Method

On April 5, 2011, when the tunnel face of the headrace tunnel 3[#] was excavated westward to Stake K6 + 152, a rock burst occurred from the south side wall to the south

Fig. 2 Relationship between the rock burst intensity classification according to the CGIHE method and the released energy monitored by the microseismic technique



spandrel of Stake K6 + 152 – 160. The rock mass in the range of the rock burst was mainly marble of the Baishan Group. The length along the tunnel axis, the width, and the maximum depth of the rock burst failure zone were approximately 8, 3, and 2 m, respectively. Because the depth of the rock burst failure zone is >1 m and <3 m, it was classified as an intense rock burst according to the CGIHE method.

According to Fig. 3, the fallen rock mass was mainly small fragments, and the failure zone, shaped by several nearly horizontal and vertical structural planes, was quite complex. This evidence showed that the initial structural planes, joints, and cracks were very rich and that the rock mass had been broken seriously before excavation in this zone. The rock fragments mainly fell near the arch foot of the tunnel, indicating that the fractured rock mass did not have sufficient kinetic energy, which was also shown by the monitored rock burst radiated energy, whose common logarithm was only $3.49 \lg(E/J)$. The investigation in situ showed that the prestressed rock bolts with a length, diameter, and spacing of 6 m, $\phi 32$ mm, and 1.0×1.0 m, respectively, and made of concrete-reinforced by steel fiber, were sprayed in the rock burst zone. However, the state of the on-site anchoring system after destruction indicates that the lack of anchoring force was mainly due to the low shear strength between the cement grout and the rod or rock mass. The low strength was related to the broken rock mass and the construction quality. Therefore, it might be better to view this failure as a collapse or a moderate rock burst than an intense rock burst.

2.4.2 Rock Burst Example II: A Moderate Rock Burst According to the CGIHE Method

On February 23, 2011, a rock burst that was 110–120 m from the tunnel face of the headrace and delayed 62 days

after the rock burst zone was excavated occurred at the south side wall of Stake K8 + 805 – 815. The involved rock mass was mainly marble of the Baishan Group. The length along the tunnel axis, the width, and the depth of the rock burst failure zone were approximately 10, 5, and 0.60 m, respectively. Because the depth of the rock burst failure zone is only >0.6 and <1 m, it was classified as a moderate rock burst according to the CGIHE method.

Figure 4 shows that there were two different characteristics that contributed to the shape of the rock burst failure zone. One characteristic was a large-scale structural plane with obvious iron and manganese rendering, parallel to the side wall; the joints and fissures were also greatly developed and rocks were broken in zone 1[#]. Another characteristic was that the failure interface was fresh with a shallow step-shape, and the breaking phenomenon was obvious close to the spandrel of the tunnel in zone 2[#]. The concrete was reinforced by steel fibers and water expansion bolts in the rock burst zone, as is also shown in Fig. 4.

Although the depth of the rock burst failure zone was shallow, the distance traveled by the ejected rock mass was far from the side wall. The farthest distance covered by the ejected rock mass was approximately 6 m from the side wall and its maximum size was approximately $0.8 \text{ m} \times 3.5 \text{ m} \times 0.5 \text{ m}$. When this rock burst occurred, the workers at the site felt the ground vibrate slightly and the common logarithm of the rockburst radiated energy as monitored by the microseismic technique reached a high value of $7.01 \lg(E/J)$. Additionally, a passing car was damaged by this rock burst, according to a worker's description. Thus, it is not reasonable to classify this rock burst as moderate according to the damage depth of 0.6 m.

The rock burst examples given above show that, although the qualitative rock burst intensity classification method is simple and convenient, it has some problems: when the engineer did not witness the entire rock burst, the

Fig. 3 Photograph after a rock burst in Stake K6 + 152–160 of 3[#] tunnel, on April 5, 2011

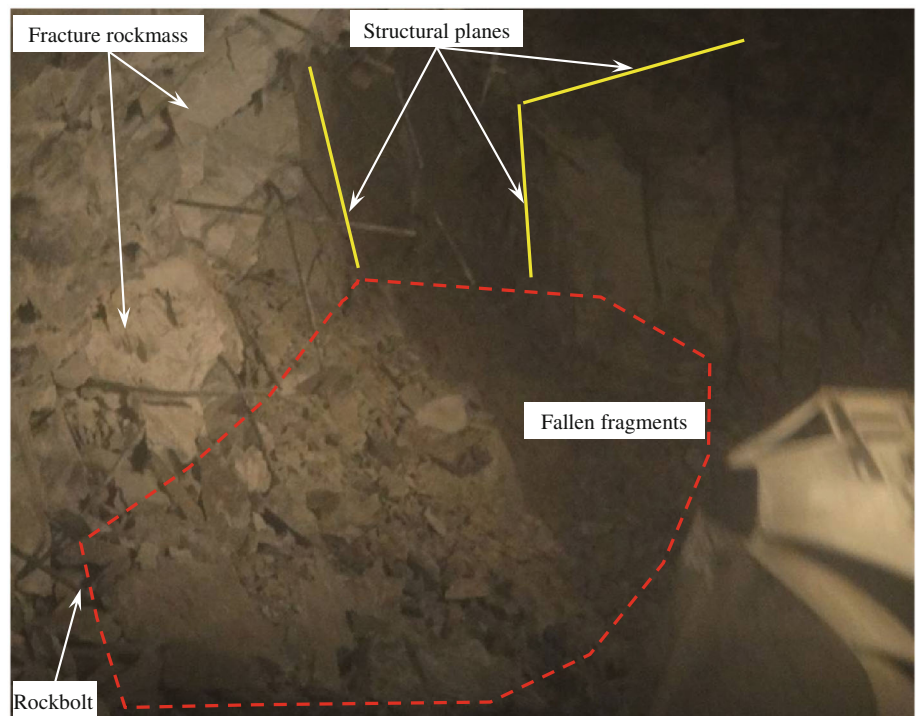
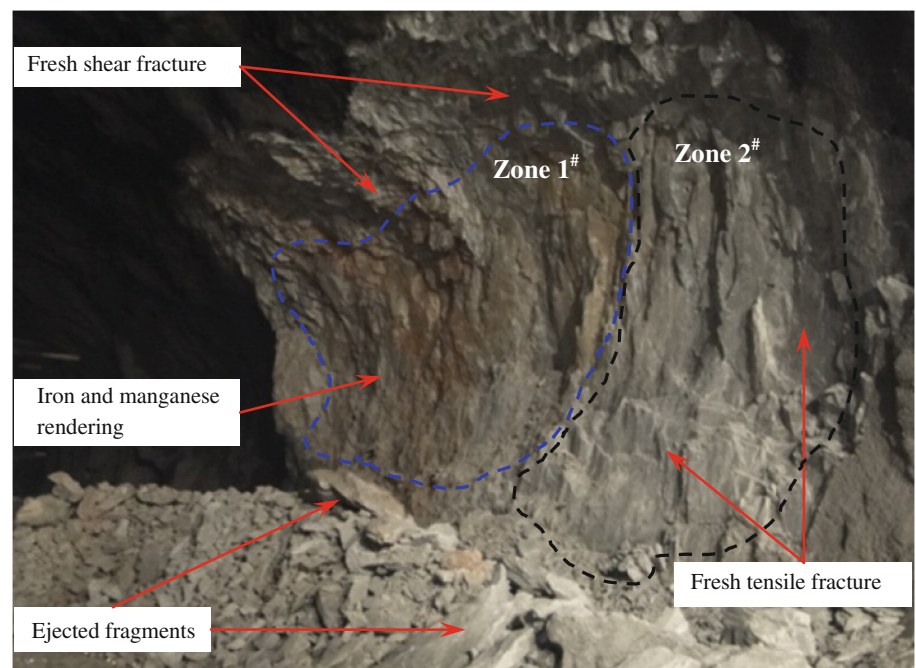


Fig. 4 Photograph after a rock burst in Stake K8 + 805–815 of 2[#] diversion tunnel, in the early morning of February 23, 2011



qualitative method to evaluate the grade of the burst comprehensively (by sound, the ejection distance of the rock fragment, the depth of the rock burst zone, and other characteristics of the event) was shifted to a classification method using only the depth of the rock burst failure zone, which resulted in some difficulties in understanding the classification result, as explained in the two rockburst examples above. In addition, due to the differences in the

knowledge of the rock bursts and the observed phenomena for different engineers at the site, the same rock burst may be classified at different grades according to different engineers, which is a disadvantage in the assessment and prevention of rock bursts. In this paper, a new quantitative classification method for rock burst intensity will be proposed in terms of radiated energy and surrounding rock damage severity.

3 A Rock Burst Intensity Quantitative Classification Method in Terms of Radiated Energy and Damage Severity

Based on the recorded energies of 133 rock bursts monitored by the microseismic technique, a new rock burst intensity quantitative classification method (RBQC method) is proposed using the hierarchical clustering analysis technique. Additionally, a new set of criteria for the quantitative classification of rock burst intensity is established on the basis of radiated energy and surrounding rock damage severity.

3.1 Classification Index

As is commonly understood, the magnitude of an earthquake is classified mainly on the basis of the earthquake’s radiated energy, and the magnitude of the earthquake increases with an increase of the radiated energy. Generally speaking, if the magnitude of the earthquake is greater, the destruction caused by the earthquake is greater; that is, the earthquake intensity is greater. As earthquake intensity levels are affected by magnitude, the epicentral distance, the depth of the hypocenter, the geological structure, the hypocenter mechanism, the characteristic of the buildings, and the rock and soil properties in the earthquake zone and so on, the magnitude and intensity of the earthquake are not in direct proportion.

The rock burst, which is a shallow-source and small-volume failure that generally occurs inside the failure zone, is greatly different from the earthquake, which is a deep-source and large-scale destructive event that occurs in the deep earth. Thus, under the same project zone with the same the geological structure and rock properties, the intensity of a rock burst and its radiated energy can be assumed to be in direct proportion.

A rock burst is a dynamic disaster. In general, when a rock burst occurs, a great amount of energy is radiated. Thus, it is possible to obtain the radiated energy of a rock burst with microseismic monitoring equipment and to classify the rock burst intensity level in terms of the radiated energy. Therefore, radiated energy can be chosen as a rock burst intensity classification index.

3.2 Classification Criteria of Rock Burst Intensity

Rock burst intensity is mainly clustered according to “distance,” which is an evaluation index difference between one rock burst and another found by utilizing the hierarchical clustering analysis technique. There are four commonly used measurement methods for distance (Ketchen and Shook 1996): the Manhattan distance, the Euclidean distance, the Minkowski distance, and the

Chebyshev distance. They can be expressed as a united Minkowski distance according to Eq. (1).

$$d_{ij}(q) = \left(\sum_{a=1}^p |x_{ia} - x_{ja}|^q \right)^{1/q}, \tag{1}$$

where x_{ia} and x_{ja} are the a th evaluation index of the rock burst i and the rock burst j , respectively, d_{ij} is the “distance” between the rock burst i and the rock burst j , p is the number of evaluation indexes of the each rock burst and q is a constant variable. The Minkowski distance is typically used with a q of 1 or 2. The latter is the Euclidean distance and the former is sometimes known as the Manhattan distance. In the limiting case of p reaching infinity, one obtains the Chebyshev distance.

In this paper, because the evaluation index of the rock burst contains only the radiated energy (p is equal to 1), it is easily proved that the four methods available to calculate the distance are the same. Thus, the Euclidean distance was selected here. The “distance” was considered the radiated energy difference between two rock bursts.

The linkage criteria determined the distance between the sets of rock bursts as a function of the pairwise distance between the bursts. Some commonly used linkage criteria between two sets of rock bursts are the single linkage method, the complete linkage method, and the Ward’s criterion (Ward 1963; Székely and Rizzo 2005), which are described in Eqs. (2), (3) and (4), respectively.

$$D_{ij}^{\min} = \min_{i \in G_i, j \in G_j} d_{ij}, \tag{2}$$

where G_i and G_j are rock burst set i and j , respectively, D_{ij}^{\min} is the minimum “distance” between G_i and G_j , and d_{ij} is the “distance” between the i th rock burst sample in G_i and the j th rock burst sample in G_j .

$$D_{ij}^{\max} = \max_{i \in G_i, j \in G_j} d_{ij}, \tag{3}$$

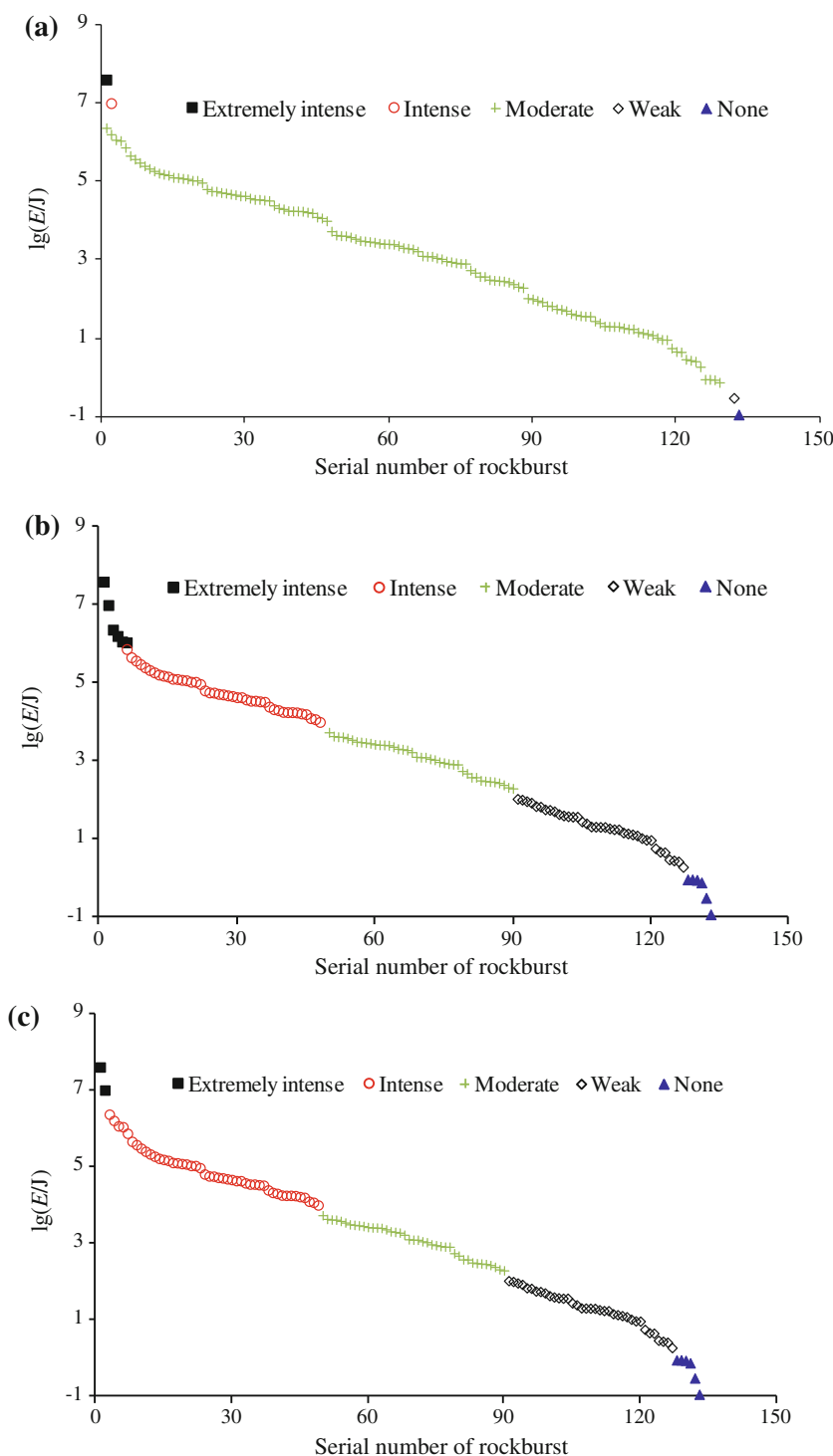
where D_{ij}^{\max} is the maximum “distance” between G_i and G_j .

$$S = \sum_{t=1}^k \sum_{i=1}^{n_t} (\mathbf{x}_i^{(t)} - \overline{\mathbf{x}}^{(t)})' (\mathbf{x}_i^{(t)} - \overline{\mathbf{x}}^{(t)}), \tag{4}$$

where N rock bursts are divided into k sets: G_1, G_2, \dots, G_k , $\mathbf{x}_i^{(t)}$. A p dimensional vector contains the evaluation indexes of the i th rock burst in set G_t , n_t is the number of rock bursts in set G_t , $\overline{\mathbf{x}}^{(t)}$ is the mean value of the evaluation indexes of the rock bursts in set G_t and S is the sum of the deviation square of the rock burst evaluation index. If S is a minimum, the sets of rock bursts are identified correctly.

One hundred and thirty-three rock bursts recorded at the Jinping II hydropower station were used as data to choose the optimal linkage criterion. The rock burst

Fig. 5 Rock burst intensity classifications using the hierarchical clustering analysis technique with different linkage criteria based on 133 rock bursts in the Jinping hydropower station, China: **a** single linkage; **b** Ward’s criterion; **c** complete linkage



intensity was classified into five levels: extremely intense, intense, moderate, weak, and none, using the hierarchical clustering analysis technique with the three linkage criteria mentioned above, as shown in Fig. 5. The number of rock bursts and percent of each level are listed in Table 3, where N is the rock burst number in each intensity level, P is the percentage of rock bursts of each classification compared with all classifications, and $\lg(E/J)$ is the

average common logarithm of the radiated energy. Using the single-linkage method, 97 % of the rockbursts were identified as moderate intensity, while the extremely intense, intense, weak, and 'none' categories comprised the remaining 3 %. This finding represents an unreasonable cluster, whether theoretical or actual. The main difference in the rock burst intensity classification according to the complete-linkage approach and the Ward’s criterion

Table 3 Rock burst intensity classifications using the hierarchical clustering analysis technique with different linkage criteria

Rock burst levels	Single linkage			Ward’s criterion			Complete linkage		
	<i>N</i>	<i>P</i> (%)	lg(<i>E</i> / <i>J</i>)	<i>N</i>	<i>P</i> (%)	lg(<i>E</i> / <i>J</i>)	<i>N</i>	<i>P</i> (%)	lg(<i>E</i> / <i>J</i>)
Extreme intense	1	0.75	7.61	6	4.51	6.65	2	1.50	7.31
Intense	1	0.75	7.01	43	32.33	4.79	47	35.34	4.91
Moderate	129	96.99	3.14	41	30.83	3.08	41	30.83	3.08
Weak	1	0.75	−0.49	37	27.82	1.31	37	27.82	1.31
None	1	0.75	−0.92	6	4.51	−0.26	6	4.51	−0.26

lg (*E*/*J*) is the common logarithm of the rock burst radiated energy

is in the classification of extremely intense and intense rock bursts. Two rock bursts were classified as extremely intense according to the complete-linkage method and the average common logarithm of their radiated energy was 7.31 lg(*E*/*J*), while six rockbursts were identified as extremely intense according to the Ward’s criterion, and the average common logarithm of their radiated energy was 6.65 lg(*E*/*J*). Based on the destruction of the surrounding rock mass and the supporting system in situ, the classification of intensity as identified by the complete-linkage method, whose formula was expressed by Eq. (3), was more reasonable.

3.3 Classification Process of the RBQC Method

Assume *N* rock bursts and that each rock burst has *P* indexes to evaluate the rock burst intensity classification expressed as x_1, x_2, \dots, x_P . Then, the rock burst intensity quantitative classification method can be described as follows:

Step 1: Construct an evaluation index matrix *X* of the rock burst intensity,

$$X = \begin{bmatrix} x_{11} & \dots & x_{1P} \\ \vdots & \vdots & \vdots \\ x_{N1} & \dots & x_{NP} \end{bmatrix} \tag{5}$$

where x_{np} is the *p*th evaluation index of the *n*th rock burst.

Step 2: If the difference between the evaluation indexes is significant or different indexes have different metrics, an incorrect rock burst intensity classification often occurs. Thus, the evaluation index in Eq. (5) must be standardized. In this paper, the standardized Eq. (6) proposed by Ketchen and Shook (1996) is introduced,

$$x_{np}^* = \begin{cases} \frac{x_{np} - \bar{x}_p}{S_p} & S_p \neq 0 \\ 0 & S_p = 0 \end{cases} \tag{6}$$

in which the mean value \bar{x}_p and the standard deviation s_p of the *p*th evaluation index are equal to $\frac{1}{N} \sum_{n=1}^N x_{np}$ and

$$\sqrt{\frac{1}{N-1} \sum_{n=1}^N (x_{np} - \bar{x}_p)^2}, \text{ respectively, } n = 1, 2, \dots, N \text{ and } p = 1, 2, \dots, P.$$

Step 3: Divide the *N* rock burst intensities into *N* sets; that is, there is one and only one rock burst in each set.

Step 4: Calculate the “distance” between two rock bursts sets using Eq. (1) and construct the “distance” matrix *D* using Eq. (3). The matrix *D* is a symmetrical matrix, its diagonal value is zero and it can be expressed by Eq. (7).

$$D = \begin{bmatrix} D_{11}^{Max} & \dots & D_{1N}^{Max} \\ \vdots & \ddots & \vdots \\ D_{N1}^{Max} & \dots & D_{NN}^{Max} \end{bmatrix} \tag{7}$$

Step 5: Find the maximum “distance” in the matrix *D* and combine the two rock burst sets corresponding to the maximum “distance” found into one new rock burst set.

Step 6: If the presetting condition is met, the rock burst intensity identification can be considered complete; the identification result is then presented and explained in terms of actual rock burst. Otherwise, set *N* equal to *N* − 1 and return to step 4.

3.4 RBQC Criteria

Based on 133 rock bursts that occurred at the Jinping II hydropower station, China, rock burst radiated energy was chosen as the evaluation index to construct the clustering samples and was standardized by Eq. (6). Using the hierarchical clustering analysis technique with the complete-linkage method, as mentioned above, rock burst intensity was classified into five levels (extremely intense, intense, moderate, weak, and none), as represented by Arabic numerals 5, 4, 3, 2 and 1, respectively, and presented in Table 4.

A new set of rock burst intensity quantitative classification criteria was proposed based on the results of rock burst intensity clustering and phenomena of different classifications, which are described in Table 5. The main phenomena were described from observations made at the Jinping II hydropower station, and descriptions from CGIHE and Tang (1992) were also referenced.

Table 4 Evaluation index and rock burst intensity classifications using the hierarchical clustering analysis technique

No.	lg (<i>EJ</i>)	SD	<i>L</i>	No.	lg (<i>EJ</i>)	SD	<i>L</i>	No.	lg (<i>EJ</i>)	SD	<i>L</i>	No.	lg (<i>EJ</i>)	SD	<i>L</i>
1	7.61	2.47	5	35	4.56	0.77	4	69	3.12	-0.03	3	103	1.59	-0.89	2
2	7.01	2.14	5	36	4.54	0.76	4	70	3.11	-0.04	3	104	1.59	-0.89	2
3	6.38	1.78	4	37	4.53	0.75	4	71	3.11	-0.04	3	105	1.46	-0.96	2
4	6.22	1.69	4	38	4.41	0.68	4	72	3.07	-0.06	3	106	1.41	-0.98	2
5	6.08	1.62	4	39	4.34	0.65	4	73	3.05	-0.07	3	107	1.33	-1.03	2
6	6.06	1.60	4	40	4.32	0.63	4	74	2.99	-0.11	3	108	1.33	-1.03	2
7	5.89	1.51	4	41	4.27	0.61	4	75	2.97	-0.12	3	109	1.32	-1.03	2
8	5.68	1.39	4	42	4.27	0.61	4	76	2.95	-0.13	3	110	1.32	-1.04	2
9	5.59	1.34	4	43	4.27	0.61	4	77	2.93	-0.14	3	111	1.29	-1.06	2
10	5.50	1.29	4	44	4.26	0.60	4	78	2.93	-0.14	3	112	1.26	-1.07	2
11	5.42	1.25	4	45	4.23	0.59	4	79	2.76	-0.23	3	113	1.26	-1.07	2
12	5.35	1.21	4	46	4.22	0.58	4	80	2.70	-0.27	3	114	1.18	-1.11	2
13	5.29	1.17	4	47	4.11	0.52	4	81	2.60	-0.32	3	115	1.16	-1.13	2
14	5.23	1.14	4	48	4.09	0.51	4	82	2.60	-0.33	3	116	1.13	-1.14	2
15	5.20	1.13	4	49	4.02	0.47	4	83	2.52	-0.37	3	117	1.10	-1.16	2
16	5.18	1.11	4	50	3.75	0.32	3	84	2.50	-0.38	3	118	1.04	-1.19	2
17	5.12	1.08	4	51	3.65	0.26	3	85	2.49	-0.38	3	119	0.99	-1.22	2
18	5.12	1.08	4	52	3.64	0.26	3	86	2.48	-0.39	3	120	0.99	-1.22	2
19	5.10	1.07	4	53	3.63	0.25	3	87	2.45	-0.41	3	121	0.77	-1.34	2
20	5.08	1.06	4	54	3.60	0.23	3	88	2.40	-0.43	3	122	0.69	-1.39	2
21	5.05	1.04	4	55	3.56	0.21	3	89	2.34	-0.47	3	123	0.67	-1.40	2
22	5.04	1.04	4	56	3.51	0.18	3	90	2.31	-0.48	3	124	0.49	-1.50	2
23	4.99	1.01	4	57	3.50	0.18	3	91	2.04	-0.63	2	125	0.46	-1.51	2
24	4.82	0.92	4	58	3.49	0.17	3	92	2.02	-0.64	2	126	0.44	-1.53	2
25	4.77	0.89	4	59	3.47	0.16	3	93	1.98	-0.67	2	127	0.30	-1.61	2
26	4.77	0.88	4	60	3.44	0.15	3	94	1.95	-0.69	2	128	-0.02	-1.78	1
27	4.74	0.87	4	61	3.43	0.14	3	95	1.86	-0.74	2	129	-0.02	-1.78	1
28	4.72	0.86	4	62	3.43	0.14	3	96	1.84	-0.75	2	130	-0.03	-1.79	1
29	4.70	0.85	4	63	3.42	0.13	3	97	1.77	-0.78	2	131	-0.10	-1.83	1
30	4.68	0.84	4	64	3.38	0.11	3	98	1.76	-0.79	2	132	-0.49	-2.05	1
31	4.65	0.82	4	65	3.33	0.08	3	99	1.72	-0.81	2	133	-0.92	-2.28	1
32	4.65	0.82	4	66	3.32	0.08	3	100	1.65	-0.85	2				
33	4.59	0.79	4	67	3.30	0.06	3	101	1.62	-0.87	2				
34	4.56	0.77	4	68	3.24	0.03	3	102	1.60	-0.88	2				

lg(*EJ*) is the common logarithm of the rock burst radiated energy, *SD* is the standard data of the common logarithm of the rock burst radiated energy standardized by expression (7), and *L* is the rock burst intensity level classified by the hierarchical clustering analysis technique

3.5 Comparison of the RBQC Criteria and the CGIHE Criteria

The intensity classifications of 133 rock bursts were reevaluated by the RBQC method and the CGIHE method, and the classification results are shown in Fig. 6. There were great differences in the classification results between the RBQC method and the CGIHE method. According to the radiated energy, the CGIHE method led to confusing conclusions due to the disadvantages of the qualitative rock burst intensity classification method mentioned in Sect. 2.3, but the proposed

method was stable and reliable because it uses quantitative classification criteria, as described in Table 5.

4 Application of the RBQC Criteria at the Jinping II Hydropower Station

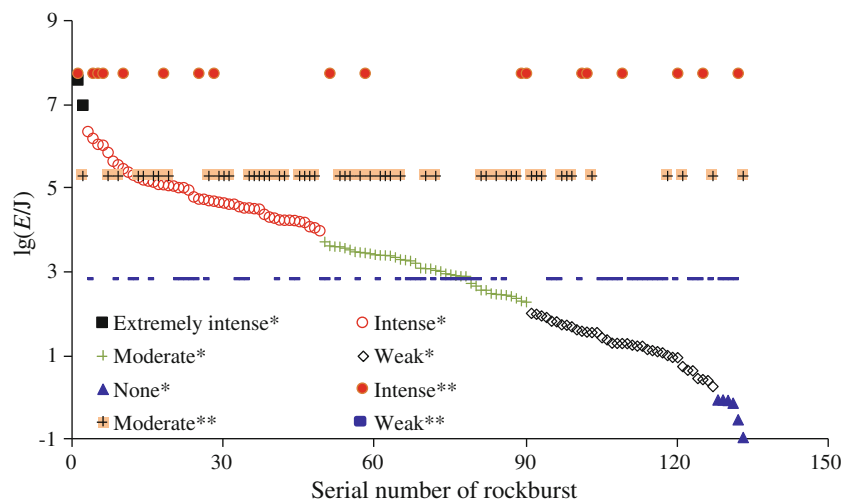
The RBQC criteria were applied during the construction of the headrace tunnels of the Jinping II hydropower station. Typical rock bursts III, IV and V, with the locations and relationships between the radiated energy and the intensity

Table 5 Rock burst intensity quantitative classification criteria based on radiated energy with rock mass failure intensity

Rock burst levels	$\lg(E/J)$	Main phenomena
None	$(-\infty, 0]$	The crack occurred inside rock mass, an obvious failure cannot be found on the surface of rock mass and the cracking sound could barely be heard. No support system and construction are affected
Weak	$(0, 2]$	Main failure type was slight spalling and slabbing in the surface of the surrounding rock mass; the rock mass was slightly ejected, the size of ejected fragment was 10–30 cm; the cracking sound could be heard slightly and the depth of failure was <0.5 m. If rock bolt and shotcrete lining are constructed in time, neither the support system nor construction are damaged
Moderate	$(2, 4]$	The main failure type was severe spalling and slabbing of the surrounding rock mass; the rock mass was obviously ejected, the size of ejected fragment was 30–80 cm; the cracking sound was like a detonator blasting and lasted for some time inside the rock mass; the failure range was obvious and the depth of failure was more than 0.5 m and <1.0 m. The shotcrete lining could be damaged among rock bolts, construction is slightly affected
Intense	$(4, 7]$	A great deal of rock mass was suddenly ejected; the failure range was extensive, the size of the ejected fragment was 80–150 cm; the edge of the failure zone typically has a fresh fracture plane; a lasting sound could be heard before rock burst; the rock burst sounded like an explosive and was louder and had an impact wave; and the depth of failure was more than 1.0 m and <2.0 m. Support system is destroyed and construction are affected
Extremely intense	$(7, +\infty]$	A large block of rock mass was suddenly ejected with intensive seismicity and the stability of the whole carve was seriously affected; the failure sound was like thunder or a cannonball and lasted a longer time; the depth of failure was more than 3.0 m, the failure ranges was more extensive, the size of the ejected rock mass was greater. Support system is seriously destroyed, and construction is seriously affected

$\lg(E/J)$ is the common logarithm of the rock burst radiated energy

Fig. 6 Comparison of the rock burst intensity classification by the RBQC criteria and the CGIHE criteria (the marks * and ** denote the results of the RBQC method and the CGIHE method, respectively)



level shown in Figs. 1b, c and 2, respectively, were selected as examples to demonstrate the feasibility and the applicability of the RBQC criteria.

4.1 Rock Burst Example III: An Extremely Intense Rock Burst

On April 16, 2011, when the tunnel face of the headrace tunnel 4[#] was excavated westward to Stake K6 + 025, a rock burst occurred in the range of Stake K6 + 025 – 045 behind the tunnel face; the location of the rock burst is shown in Fig. 1c. The workers heard a very loud sound like a cannonball and felt severe vibrations inside the tunnel. In

the process of clearing away the debris, the floor at K6 + 040 of the headrace tunnel 4[#] was found to have been uplifted with fresh rock outcrops. According to the field survey, the fresh floor strata in the 30-m range behind the face was uplifted by approximately 2 m with a 10–13-m width, slightly dipping toward the north, as shown in Fig. 7. The surrounding rock mass was broken and shotcrete was destroyed on both sides of the arch foot, but no significant deformity or damage was found in the rock bolts or shotcrete in the vault, the spandrels, or the side walls. In addition, a moderate rock burst was subsequently induced by this event in the drainage tunnel, as described by Zhang et al. (2012a).

The maximum radiated energy of this rock burst, which had a common logarithm of $7.62 \lg(E/J)$, was $4.12E + 07J$ and was thus classified as an extremely intense rock burst based on of the RBQC criteria.

4.2 Rock Burst Example IV: An Intense Rock Burst

At approximately 11 a.m. on August 12, 2011, a rock burst, with a loud sound like blasting, occurred from the north side wall to the north spandrel in the range of Stake K8 + 827 – 852 in the headrace tunnel 4[#], whose location is shown in Fig. 1c. A “V”-shaped rock burst failure zone, with a depth of approximately 1.8 m, was formed and the failure plane was fresh. Figure 8 shows that the rock bolts and shotcrete were destroyed.

Microseismic monitoring showed that the maximum radiated energy of this rock burst, which had a common logarithm of $6.22 \lg(E/J)$, was $1.66E + 06J$ and it was

subsequently classified as an intense rock burst according to the RBQC criteria.

4.3 Rock Burst Example V: A Moderate Rock Burst

At approximately 9 a.m. on June 20, 2011, a rock burst (location is shown in Fig. 1c) occurred at the south side wall in the range of Stake K5 + 623 – 628 in the headrace drainage tunnel. The main failure type was severe spalling and slabbing of the surrounding rock mass. A few rock mass fragments were ejected with a short distance, as shown in Fig. 9.

The microseismic monitoring showed that the maximum radiated energy of this rock burst, which had a common logarithm of $3.56 \lg(E/J)$, was $3.63E + 03J$ and it was thus classified as a moderate rock burst according to the RBQC criteria.

The rock burst intensity classifications above are consistent with the conclusions drawn by the rock burst

Fig. 7 An extremely intense rock burst occurred at Stake K6 + 025 – 045 in tunnel 4[#] on April 16, 2011

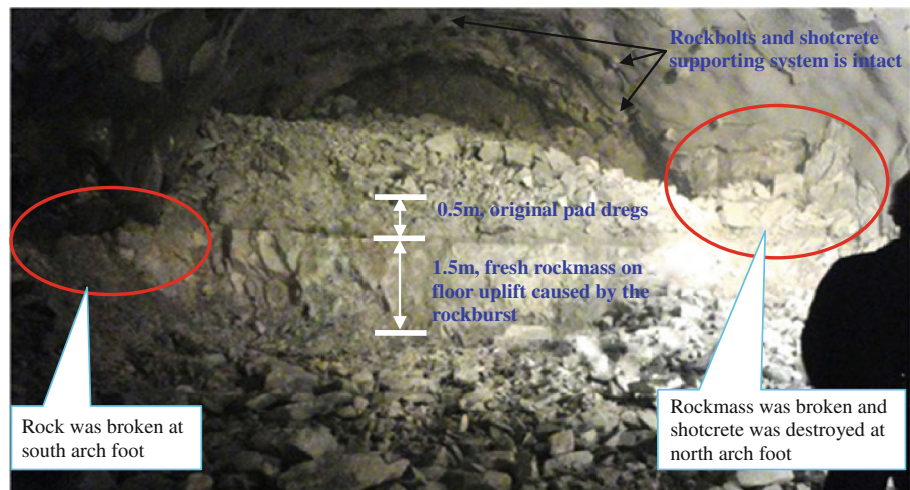


Fig. 8 An intense rock burst occurred at Stake K8 + 827 – 852 in tunnel 4[#] on August 12, 2011

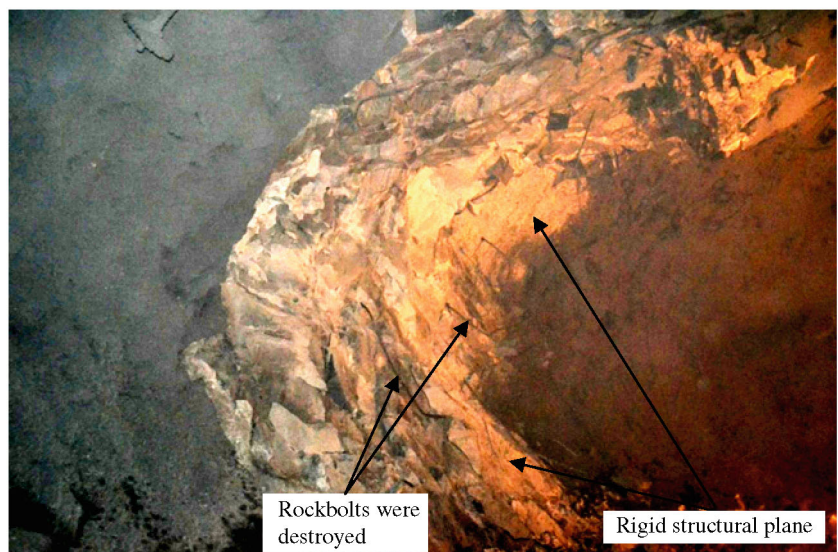




Fig. 9 A moderate rock burst occurred at Stake K5 + 623 – 628 in the drainage tunnel on June 20, 2011

prevention and control team, which consisted of professors, senior engineers, researchers and workers, after an investigation was performed in situ. The application in situ showed that the RBQC criteria had a good stability and feasibility, and could evaluate rock burst classification adequately if microseismic monitoring was performed along with the rock engineering.

5 Conclusions

Radiated energy can be viewed as a rock burst intensity evaluation index. Based on this, we proposed a quantitative classification method for rock burst intensity using the hierarchical clustering analysis technique with the complete-linkage method, as well as a new set of quantitative classification criteria for rock burst intensity, based on the radiated energy of 133 rock bursts monitored via microseismic technique at the Jinping II hydropower station, China. The new criteria classified rock burst intensity into five levels: extremely intense, intense, moderate, weak, and none, and the common logarithms of the radiated energy of each level were $>7 \lg(E/J)$, $>4 \lg(E/J)$ and $<7 \lg(E/J)$, $>2 \lg(E/J)$ and $<4 \lg(E/J)$, $>0 \lg(E/J)$ and $<2 \lg(E/J)$, and $<0 \lg(E/J)$, respectively. The application of this method to the Jinping II hydropower station showed that the proposed criterion had a good stability and feasibility, and could classify rock bursts appropriately if microseismic monitoring was conducted along with the rock engineering.

Although the proposed quantitative classification method for the rock burst intensity and the proposed criteria can be widely used for different rock engineering projects, they must be improved further because (1) good classification criteria should be tested and confirmed on a great number of rock burst examples occurring in different

rock engineering projects, and involving rock with different physical and mechanical properties; and (2) the rock burst radiated energy obtained by the microseismic technique was affected by the arrangement and the installation of the sensors, the coupling of the sensors with the rock mass, the sensitivity of the microseismic monitoring system, the energy compensation theory (as the wave passed through the rock material), the precise identification of the source location, and the source mechanism assumption.

Acknowledgments Financial support from the Special Funds for Major State Basic Research Project under Grant No. 2010CB732006, the National Natural Science Foundation of China under Grant No. 41272347, the Key Research Program of the Chinese Academy of Sciences, Grant No. KZZD-EW-05 and the Ertan Hydropower Development Co., Ltd. under Grant No. JPIIA-201004 are gratefully acknowledged. We are also grateful for the support and assistance in the headrace tunnel design and construction from the engineers at the China Railway 18 Bureau Group Co., Ltd., the Beijing Vibroflotation Engineering Co., Ltd. and the East China Investigation and Design Institute.

References

- Board MP (1994) Numerical examination of mining-induced seismicity. PhD thesis, University of Minnesota
- Brauner G (1985) Ground pressure and coal bumps (Translated by Li Y). China Coal Industry Publishing House, Beijing, pp 17–53 (in Chinese)
- Canadian Rockburst Research Program (1996) Rockburst Research Handbook: a comprehensive summary of five years of collaborative research on rockbursting in hard rock mines. CAMIRO Mining Division, CRRP
- Chen BR, Feng XT et al (2011) Real-time microseismic monitoring and its characteristic analysis during TBM tunneling in deep-buried tunnel. *Chin J Rock Mech Eng* 30(2):275–283
- Cook NGW, Hoek E, Pretorius JPG, Ortlepp WD, Salamon MDG (1966) Rock mechanics applied to the study of rockbursts. *J S Afr Inst Min Metall* 66:435–528
- Feng XT, Zhou H (2006) Research report on stability of surrounding rock mass and structure design of diversion tunnels of Jinping II hydropower station at Yalong River during invite public bidding and design phase. Institute of Rock and Soil Mechanics, Chinese Academy of Sciences
- Ge M (2005) Efficient mine microseismic monitoring. *Int J Coal Geol* 64:44–56
- He MC, Miao JL, Feng JL (2010) Rock burst process of limestone and its acoustic emission characteristics under true-triaxial unloading conditions. *Int J Rock Mech Min Sci* 47:286–298
- Huang SL (2008) Study on mechanical model of brittle rock under high stress condition and its engineering applications. PhD thesis, Institute of Rock and Soil Mechanics, the Chinese Academy of Sciences, China (in Chinese)
- Jiang Q, Feng XT, Xiang TB, Su GS (2010) Rockburst characteristics and numerical simulation based on a new energy index: a case study of a tunnel at 2,500 m depth. *Bull Eng Geol Environ* 69:381–388
- Ketchen DJ Jr, Shook CL (1996) The application of cluster analysis in strategic management research: an analysis and critique. *Strateg Manag J* 17:441–458
- Kostrov BV (1974) Seismic moment and energy of earthquakes and seismic flow of rock. *Izv Phys Solid Earth* 13:13–21

- Luo X, Creighton A, Gough J (2010) Passive seismic monitoring of mine-scale geothermal activity: a trial at Lihir open pit mine. *Pure Appl Geophys* 167:119–129
- Milev AM, Spottiswoode SM, Rorke AJ (2001) Seismic monitoring of a simulated rockburst on a wall of an underground tunnel. *J S Afr Inst Min Metall* 101:253–260
- National Standards Compilation Group of People's Republic of China (2008) Code for geological investigation on hydropower engineering. China Planning Press, Beijing (in Chinese)
- Ortlepp WD, Stacey TR (1994) Rockburst mechanisms in tunnels and shafts. *Tunn Undergr Space Technol* 9:59–65
- Rudnicki JW, Freund LB (1981) On energy radiation from seismic sources. *Bull Seism Soc Am* 71:583–595
- Russnes BF (1974) Analyses of rockburst in tunnels in valley sides [MSc. Thesis] [D]. Norwegian Institute of Technology, Trondheim, pp 247–247
- Shan Z, Yan P (2010) Management of rock bursts during excavation of the deep tunnels in Jinping II Hydropower Station. *B Eng Geol Environ* 69:353–363
- Snelling PE, Godin L, McKinnon SD (2013) The role of geologic structure and stress in triggering remote seismicity in Creighton Mine, Sudbury, Canada. *Int J Rock Mech Min Sci* 58:166–179
- Székely GJ, Rizzo ML (2005) Hierarchical clustering via joint between-within distances: extending Ward's minimum variance method. *J Classif* 22:151–183
- Tang Y (1992) A new classification of rockburst intensity. *Geol Rev* 38(5):439–443
- Tang BY (2000) Rockburst control using distress blasting. PhD thesis, McGill University, Montreal, Canada
- Ward JH (1963) Hierarchical grouping to optimize an objective function. *J Am Stat Assoc* 58(301):236–244
- Wu S, Shen M, Wang J (2010) Jinping hydropower project: main technical issues on engineering geology and rock mechanics. *B Eng Geol Environ* 69:325–332
- Young RP, Collins DS (2001) Seismic studies of rock fracture at the Underground Research Laboratory, Canada. *Int J Rock Mech Min Sci* 38:787–799
- Zhang CQ, Feng XT, Zhou H, Qiu SL, Wu WP (2012a) Case histories of four extremely intense rockbursts in deep tunnels. *Rock Mech Rock Eng* 45:275–288
- Zhang CQ, Feng XT, Zhou H (2012b) A top pilot tunnel preconditioning method for the prevention of extremely intense rockbursts in deep tunnels excavated by TBMs. *Rock Mech Rock Eng* 45:289–309